Intermetallics 96 (2018) 90–93

Contents lists available at ScienceDirect

Intermetallics

journal homepage: www.elsevier.com/locate/intermet

Distinct spin glass behavior and excellent magnetocaloric effect in $Er_{20}Dy_{20}Co_{20}Al_{20}RE_{20}$ (RE = Gd, Tb and Tm) high-entropy bulk metallic glasses

Jun Li[a,b], Lin Xue[a,b], Weiming Yang[b,c], Chenchen Yuan[a,b], Juntao Huo[d], Baolong Shen[a,b,c,*]

[a] School of Materials Science and Engineering, Southeast University, Nanjing, 211189, China
[b] Jiangsu Key Laboratory for Advanced Metallic Materials, Nanjing, 211189, China
[c] Institute of Massive Amorphous Metal Science, China University of Mining and Technology, Xuzhou, 221116, China
[d] Key Laboratory of Magnetic Materials and Devices, Ningbo Institute of Materials Technology & Engineering, Chinese Academy of Sciences, Ningbo, 315201, China

ARTICLE INFO

Keywords:
RE-based high-entropy bulk metallic glasses
Spin glass
Magnetocaloric effect
Refrigerant capacity

ABSTRACT

The $Er_{20}Dy_{20}Co_{20}Al_{20}RE_{20}$ (RE = Gd, Tb and Tm) high-entropy bulk metallic glasses (HE BMGs) with tunable magnetocaloric properties were prepared successfully. As a result, a spin glass behavior was observed below 50 K in this HE BMG system. In addition, we found that the Curie temperature (T_C) can be easily tuned from 13 to 43 K by alloying different rare earth (RE) elements, following a good de Gennes factor dependence. The peak of magnetic entropy change ($|\Delta S_M^{max}|$) for Gd-, Tb- and Tm-containing glassy alloy under a magnetic field of 5 T is 9.1, 8.6 and 11.9 J kg^{-1}K^{-1}, respectively, which leads to obtain the maximum refrigerant capacity (*RC*) of 619, 525, and 405 J kg^{-1} for the $Er_{20}Dy_{20}Co_{20}Al_{20}RE_{20}$ (RE = Gd, Tb and Tm) HE BMGs, respectively. The glass-forming ability (GFA), T_C, ΔS_M and *RC* can be widely tuned by alloying different RE elements. These results suggest that these HE BMGs are promising magnetic refrigerants at low temperature in the future.

1. Introduction

Very recently, the high-entropy alloys (HEAs), a kind of new material in alloy design that consists of five or more principal elements with equal or nearly equal atomic percentage, have attracted increasing concerns in both fundamental sciences and engineering applications due to their multiple compositions, complicated microstructures and adjustable properties including high corrosion resistance, abrasive resistance, and high strength even at elevated temperature [1–4]. In addition, bulk metallic glasses (BMGs) also exhibit superior properties compared with crystalline materials, such as the tailorable Curie temperature (T_C), the higher electrical resistivity and broad magnetic entropy change (ΔS_M) peak, therefore hold promises for a variety of applications [4–6]. Given the unique characteristics and excellent properties of the two kinds of materials mentioned above, formation of the HEAs with amorphous structures, that is HE BMGs, provides new possibilities in developing alloys with the advantages of both HEAs and BMGs [4,5]. The HE BMGs have shown unique and remarkably improved properties due to the strong topological and chemical disorder, compared with the normal BMGs and HEAs [4–8]. Therefore, a large number of HE BMGs have been prepared and studied because they might be of great importance for future applications. For example, the $Ti_{20}Zr_{20}Hf_{20}Be_{20}Ni_{20}$ HE BMG exhibits high yield strength, together with the relatively large plastic strain up to 4% with a critical size of 15 mm [5]. The $Ca_{20}Mg_{20}Zn_{20}Sr_{20}Yb_{20}$ HE BMG with enhanced mechanical properties and corrosion resistance is more suitable for biomedical applications, compared to the CaMgZn BMGs [9].

However, up to now, most researches mainly focus on mechanical properties, and only a little work has been carried out on magnetic properties, especially the magnetocaloric properties in HE BMGs. Since the discovery of giant magnetocaloric effect (GMCE) in $Gd_5Si_2Ge_2$, increasing concerns have been put into the development of magnetic refrigerants [10,11]. In the past decades, a number of magnetic materials have been reported to exhibit large MCE [12–14]. Due to the profuse magnetic structure of RE elements, a series of heavy RE-(Gd, Ho, Dy, Er and Tb) based glassy alloys have been extensively studied, which exhibits large MCE and shows the potential applications [15–19]. Furthermore, spin glass (SG) behavior below the freezing temperature (T_f) was observed and discussed in these alloys. Recently, $Ho_{20}Er_{20}Co_{20}Al_{20}RE_{20}$ (RE = Gd, Dy, and Tm) HE BMGs were prepared successfully with excellent MCE and distinct SG behavior, which provides a new research direction of HE BMGs [6]. However, the $Ho_{20}Er_{20}Co_{20}Al_{20}RE_{20}$ (RE = Gd, Dy, and Tm) HE BMGs show low glass-forming ability (GFA) and T_C, which limits the development and

* Corresponding author. School of Materials Science and Engineering, Southeast University, Nanjing, 211189, China.
E-mail address: blshen@seu.edu.cn (B. Shen).

https://doi.org/10.1016/j.intermet.2018.03.002
Received 18 October 2017; Received in revised form 10 January 2018; Accepted 5 March 2018
Available online 20 March 2018
0966-9795/

potential applications as magnetic refrigerants. Moreover, only a little work focus on the MCE of HE BMGs containing three kinds of RE elements.

In this paper, the pentabasic $Er_{20}Dy_{20}Co_{20}Al_{20}RE_{20}$ (RE = Gd, Tb and Tm) BMGs were designed and prepared, a distinct SG behavior, combined with improved GFA and excellent MCE were obtained in this glassy alloy system. The effects of RE on the GFA, SG behavior, T_C, ΔS_M, and refrigerant capacity (*RC*) were systematically investigated and discussed.

2. Experimental

The HEA ingots with the following nominal compositions $Er_{20}Dy_{20}Co_{20}Al_{20}RE_{20}$ (RE = Gd, Tb and Tm) were prepared by arc melting highly pure elements (Er: 99.9 wt %, Dy: 99.9 wt %, Co: 99.99 wt %, Al: 99.9 wt %, Gd: 99.9 wt %, Tb: 99.9 wt %, Tm: 99.9 wt %) in a Ti-gettered argon atmosphere. The alloy ingots were remelted five times to ensure homogeneity. The as-cast rods with diameters of 1 mm and 1.5 mm were prepared by Cu mold suction casting method under argon atmosphere. The amorphous nature of the as-cast rods which was ground into powder was ascertained by X-ray diffraction (XRD) with Cu Kα radiation (2θ = 20–90°). The thermal analysis was carried out by differential scanning calorimeter (DSC) with a heating rate of 40 K/min using the BMGs with diameter of 1 mm. The temperature and field dependences of magnetization were measured by a SQUID magnetometer through field cooling magnetization (M_{FC}) and zero field cooling magnetization (M_{ZFC}). The M_{FC} was measured under an applied magnetic field of 16 kA m^{-1} on heating course after initially cooling the BMG with diameter of 1 mm from 120 to 2 K under the same field. The M_{ZFC} was measured on the heating course under the same field of M_{FC} after initially cooling from 120 to 2 K without applied magnetic field. The isothermal magnetization (*M-H*) curves were measured with magnetic field up to 5 T, and the temperature intervals of 3 and 10 K were selected for the regions in the vicinity of T_C and far away from T_C, respectively.

3. Results and discussion

Fig. 1 shows the XRD patterns of the as-cast $Er_{20}Dy_{20}Co_{20}Al_{20}RE_{20}$ (RE = Gd, Tb and Tm) alloys with diameters of 1 mm and 1.5 mm. Only broad peaks can be seen for metallic alloys with compositions of $Er_{20}Dy_{20}Co_{20}Al_{20}RE_{20}$ (RE = Gd, Tb and Tm) illustrating the formation of a fully glassy structure in the diameter range up to at least 1 mm. On the other hand, the alloys containing Gd and Tb with a diameter of 1.5 mm show fully glassy structure based on the XRD patterns, which means that the elements Gd and Tb have a positive influence on the GFA of this alloy system. The DSC curves of the as-cast $Er_{20}Dy_{20}Co_{20}Al_{20}RE_{20}$ (RE = Gd, Tb and Tm) HE BMGs are shown in Fig. 2. It is seen that all the alloys exhibit an obvious endothermic reaction due to glass transition and exothermic peak related to crystallization, which means the formation of glassy alloys. The values of transition temperature (T_g), crystallization temperature (T_x) and supercooled liquid region ($\triangle T_x = T_x - T_g$) have been summarized in Table 1. Both of the T_g and T_x increase gradually in terms of the sequence of the Gd, Tb and Tm, this indicates an increase in the thermal stability of the supercooled liquid [20]. Therefore, it is considered that the thermal stability of this glassy alloy system increases in terms of the sequence of the Gd, Tb and Tm. It was found that electrons could transfer from the metalloid elements to fill the *d* shells in the transition metal elements to form a *s-d* hybrid bonding [21]. In this study, the numbers of 4*f* band electrons in Gd, Tb and Tm elements are 7, 9 and 13, respectively. Consequently, it is considered that the *f-d* hybrid bonding nature between RE and Co elements would increases in terms of the sequence of the Gd, Tb and Tm, which results in an increase of thermal stability of the supercooled liquid.

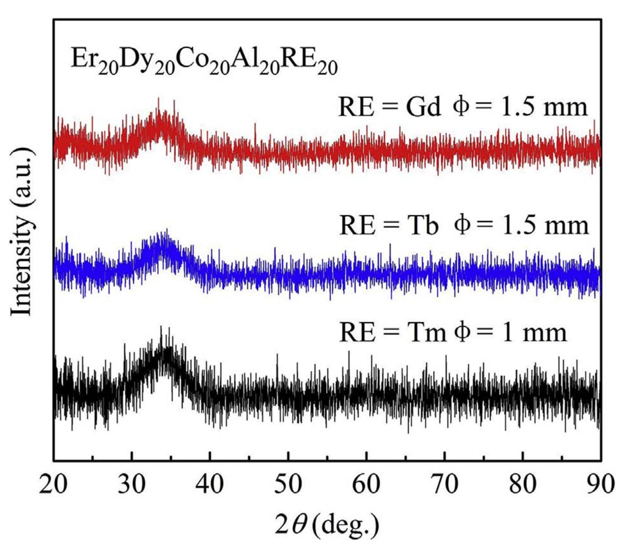

Fig. 1. XRD patterns of the as-cast $Er_{20}Dy_{20}Co_{20}Al_{20}RE_{20}$ (RE = Gd, Tb and Tm) rods with diameter of 1 mm and 1.5 mm.

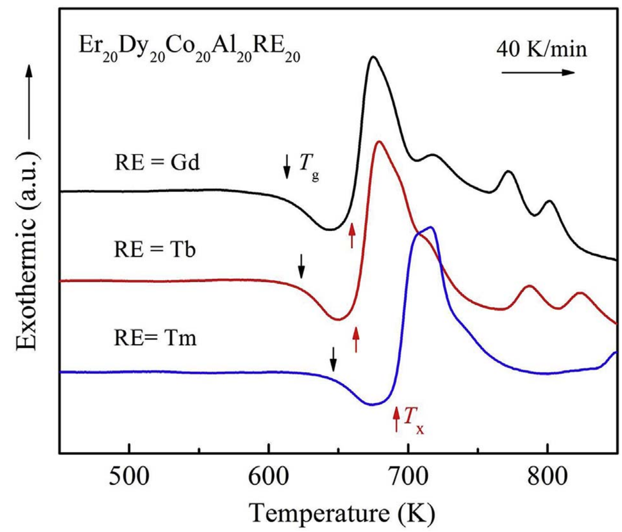

Fig. 2. DSC curves of the as-cast $Er_{20}Dy_{20}Co_{20}Al_{20}RE_{20}$ (RE = Gd, Tb and Tm) HE BMGs.

Fig. 3 shows the M_{FC} and M_{ZFC} curves for the as-cast $Er_{20}Dy_{20}Co_{20}Al_{20}RE_{20}$ (RE = Gd, Tb and Tm) HE BMGs. For each alloy, a spin freezing transition can be observed, while a cusp exists in the M_{ZFC} curve at the same temperature where a divergence appears between the M_{FC} and M_{ZFC} curves, which is a typical SG-like behavior. This is different from some glassy alloys, such as most Gd-based MGs which generally show ferromagnetic transition due to the absence of orbital momentum of Gd [16,22]. The reason is that the exchange interactions dominate the magnetic behavior in these Gd-based MGs, while the random magnetic anisotropy arising from the local random electrostatic field plays a significant role in this RE based HE BMGs [16,23]. The T_C of $Er_{20}Dy_{20}Co_{20}Al_{20}RE_{20}$ (RE = Gd, Tb and Tm) HE BMGs calculated from the differentiation of M_{FC} curves are 43, 29 and 13 K for RE = Gd, Tb and Tm, respectively, marked by arrows in the insert of Fig. 3. Generally, the T_C usually tends to follow the de Gennes factor (*F*) in the RE-based metallic glasses [24], i.e., the larger the magnitude of *F*, the greater the value of T_C. The *F* can be expressed as: $F = J(J+1)(g-1)^2$ [25], where *J* (*J* = 3.5, 6, and 6 for RE = Gd, Tb and Tm, respectively) represents the total orbital quantum number, and *g* represents the gyromagnetic ratio given by $g = 1 + [J(J+1) + S(S+1) - L(L+1)]/2J(J+1)$, where *S* (*S* = 3.5, 3, and 1 for RE = Gd, Tb and Tm, respectively) represents the spin

Table 1
The thermal parameters and magnetocaloric properties under an applied magnetic field of 5 T of as-cast $Er_{20}Dy_{20}Co_{20}Al_{20}RE_{20}$ (RE = Gd, Tb and Tm) HE BMGs.

Composition	T_g (K)	T_x (K)	$\triangle T_x$ (K)	T_C (K)	T_f (K)	$\lvert\Delta S_M^{max}\rvert$ (J kg^{-1}K^{-1})	δT_{FWHM} (K)	RC (J kg^{-1})	Ref.
$Er_{20}Dy_{20}Co_{20}Al_{20}Gd_{20}$	610	659	49	43	36	9.1	68	619	This work
$Er_{20}Dy_{20}Co_{20}Al_{20}Tb_{20}$	623	663	40	29	24	8.6	61	525	This work
$Er_{20}Dy_{20}Co_{20}Al_{20}Tm_{20}$	645	690	45	13	11	11.9	34	405	This work
$Ho_{20}Er_{20}Co_{20}Al_{20}Gd_{20}$	612	652	40	37	–	11.2	56	627	6
$Ho_{20}Er_{20}Co_{20}Al_{20}Dy_{20}$	632	668	36	18	–	12.6	37	468	6
$Ho_{20}Er_{20}Co_{20}Al_{20}Tm_{20}$	648	680	32	9	–	15.0	25	375	6
$Gd_{20}Tb_{20}Dy_{20}Ni_{20}Al_{20}$	582	607	25	45	–	7.25	70	507	7
$Tb_{55}Co_{20}Al_{25}$	614	680	66	105	–	7.5	47	352	16
$Er_{50}Y_{26}Co_{24}Al_6$	651	702	51	8	–	15.9	27	423	17
$Dy_{36}Ho_{20}Co_{20}Al_{24}$	633	687	54	23	–	9.49	44	417	18

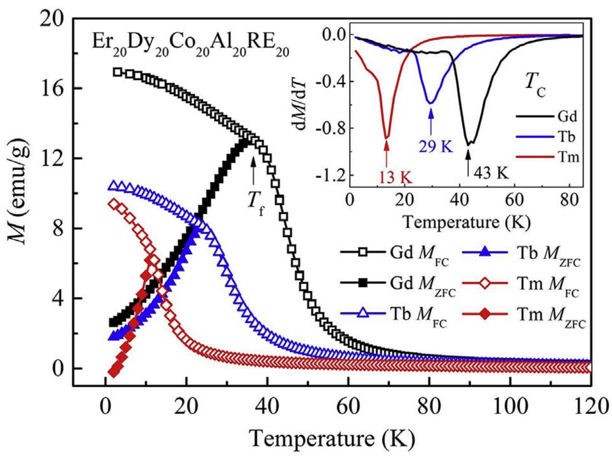

Fig. 3. The M_{FC} and M_{ZFC} curves for the as-cast $Er_{20}Dy_{20}Co_{20}Al_{20}RE_{20}$ (RE = Gd, Tb and Tm) HE BMGs. The insert shows the curves of dM/dT versus temperature.

quantum number and L (L = 0, 3, and 5 for RE = Gd, Tb and Tm, respectively) represents the orbital angular momentum quantum number. The F of Gd, Tb, and Tm obtained by theoretical calculation are 15.8, 10.5 and 1.2, respectively. It is consistent with experiment result as shown in Fig. 3 that the Gd-containing glassy alloy exhibits the highest T_C. Thus, the de Gennes factor is a good guide for estimating the T_C in a given lanthanide compound series.

Fig. 4 shows a set of isothermal magnetization curves for $Er_{20}Dy_{20}Co_{20}Al_{20}Gd_{20}$ HE BMG as an example. The magnetization of these glassy alloys rises abruptly at low magnetic field and temperature

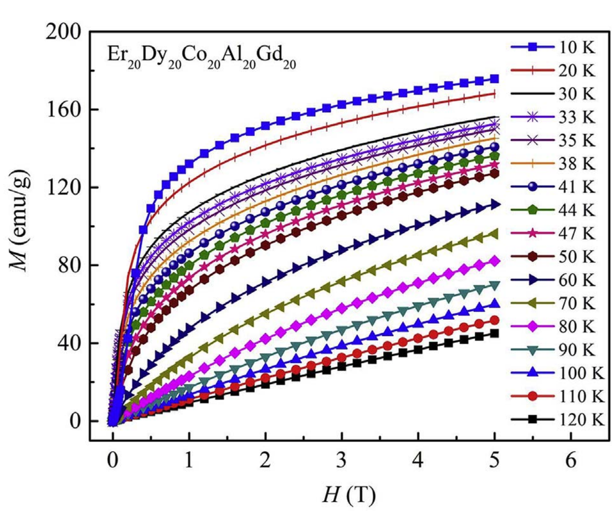

Fig. 4. Isothermal magnetization curves of the as-cast $Er_{20}Dy_{20}Co_{20}Al_{20}Gd_{20}$ HE BMG as an example.

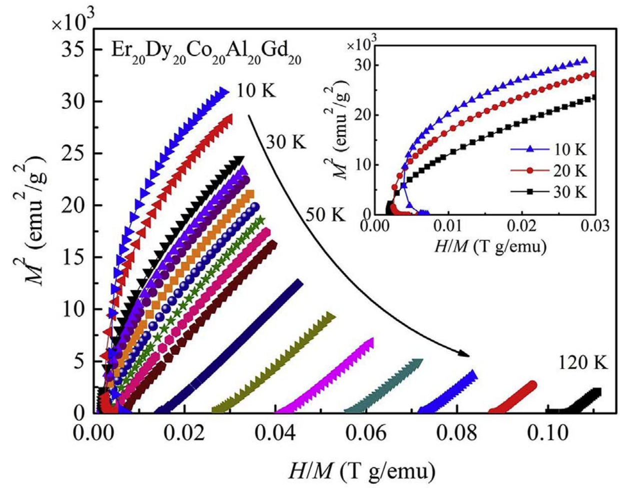

Fig. 5. The Arrott plots for the as-cast $Er_{20}Dy_{20}Co_{20}Al_{20}Gd_{20}$ HE BMG. The insert is Arrott plots for the as-cast $Er_{20}Dy_{20}Co_{20}Al_{20}Gd_{20}$ HE BMG at 10, 20, and 30 K, respectively.

below T_C, and then rapidly reaches saturation, showing obvious ferromagnetic behavior. In addition, the curves gradually turn to straight lines due to the change from ferromagnetic to paramagnetic with the increasing temperature. Fig. 5 shows the Arrott plots for the as-cast $Er_{20}Dy_{20}Co_{20}Al_{20}Gd_{20}$ HE BMG between 10 and 120 K and the insert is the selected Arrott plots at temperature for 10, 20, and 30 K, respectively. Based on the magnetism, the magnetic transition is classified to first order when the slope of Arrott plot is negative; otherwise, it is classified to second order when the slope is positive [26]. It is noted that negative slope is obviously observed in the S-shape curves below the T_f, and the inflection point corresponding to the value of H/M is enhanced with decreasing temperature, as shown in the insert of Fig. 5, which can be attributed to the SG behavior of the alloy [15,27,28]. Additionally, positive slopes without inflection point are observed above T_f, demonstrating a second order magnetic transition in the $Er_{20}Dy_{20}Co_{20}Al_{20}Gd_{20}$ HE BMG.

The magnetic entropy change ΔS_M is an important parameter to evaluate the MCE of these HE BMGs. In an isothermal process of magnetization, the ΔS_M of the system caused by a magnetic field can be given by integrating the Maxwell relation over the magnetic field [15].

$$\Delta S_M(T, H) = S_M(T, H) - S_M(T, 0) = \int_{H_0}^{H_{max}} \left(\frac{\partial M}{\partial T}\right) dH \quad (1)$$

where H_{max} and H_0 represent the maximum and minimum value of the magnetic fields. In this work, H_{max} and H_0 are 5 T and 0 T, respectively. Fig. 6 shows ΔS_M as a function of the temperature under an applied filed of 5 T for HE BMGs. It is worthy to note that the $\lvert\Delta S_M^{max}\rvert$ is observed near T_C, which can be attributed to the transition from ferromagnetism to paramagnetism. The values of $\lvert\Delta S_M^{max}\rvert$ are 9.1, 8.6 and 11.9 J kg^{-1}K^{-1} for HE BMGs with RE = Gd, Tb and Tm, respectively,

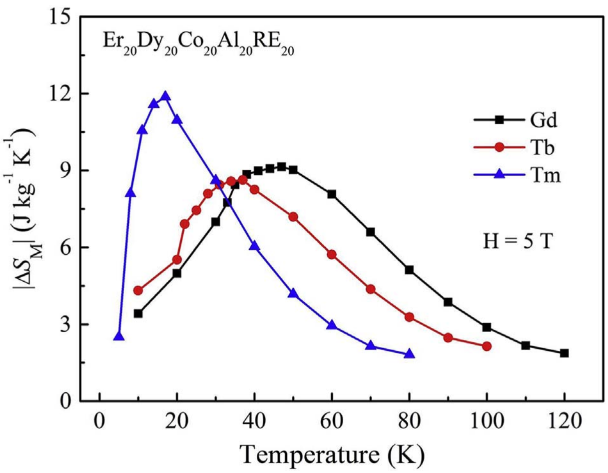

Fig. 6. The magnetic entropy change ΔS_M of the as-cast $Er_{20}Dy_{20}Co_{20}Al_{20}RE_{20}$ (RE = Gd, Tb and Tm) HE BMGs as a function of temperature under an applied field of 5 T.

demonstrating their excellent MCE.

The *RC* is another key parameter to evaluate the magnetic refrigerants, which is proportional to the area under the curve of ΔS_M versus *T*. The *RC* estimated using Gschneidner method [29] can be expressed as:

$$RC = |\Delta S_M^{max}| \times \delta T_{FWHM} \quad (2)$$

where δT_{FWHM} presents the full width at half maximum of $|\Delta S_M|$. As shown in Table 1 and Fig. 6, the δT_{FWHM} values under an applied magnetic field of 5 T are 68, 61 and 34 K for these HE BMGs with RE = Gd, Tb and Tm, respectively. In addition, the *RC* values for these HE BMGs are 619, 525 and 405 J kg^{-1} with RE = Gd, Tb and Tm, respectively. All the alloys have a large *RC* value compared to other RE-based BMGs as listed in Table 1. It is noted that the $Er_{20}Dy_{20}Co_{20}Al_{20}Gd_{20}$ HE BMG has the largest *RC* among these three alloys for its widest δT_{FWHM}, though the $Er_{20}Dy_{20}Co_{20}Al_{20}Tm_{20}$ HE BMG exhibits the largest $|\Delta S_M^{max}|$. The high *RC* should be attributed to the large ΔS_M and the particular glassy and magnetic structure which extends the large ΔS_M to a wider temperature range. In the SG alloy, magnetic moments are frozen into the equilibrium orientation, but there is no long-range order, which makes it more difficult to be frozen than the ferromagnetic alloys [6,30]. Therefore, the magnetic transition temperature range can be effectively widened due to the SG behavior and complicated compositions, which can broaden the full width at δT_{FWHM} and improve the *RC* [6]. The large magnetic entropy change ΔS_M and excellent *RC*, accompanying the inherent amorphous nature, make the HE BMGs promising magnetic refrigerant materials in helium and hydrogen liquefaction temperature range.

4. Conclusions

In this work, $Er_{20}Dy_{20}Co_{20}Al_{20}RE_{20}$ (RE = Gd, Tb and Tm) HE BMGs were prepared with larger GFA and tunable magnetocaloric properties. Distinct SG behaviors were observed among these BMGs, which are more apparent than some RE-based BMGs. The values of T_C are 43, 29 and 13 K with RE = Gd, Tb and Tm, respectively, following a good de Gennes factor dependence. The large $|\Delta S_M^{max}|$ of 11.9 J kg^{-1}K^{-1} and *RC* of 619 J kg^{-1} are obtained for RE = Tm and Gd, respectively. The excellent MCE and moderate GFA make these HE BMGs promising candidate refrigerants in helium and hydrogen liquefaction temperature range. The exploration of these HE BMGs provides more ideas for understanding magnetic behavior of BMGs.

Acknowledgments

This work was supported by the National Natural Science Foundation of China (Grant Nos. 51631003, 51471050 and 51601038), the Natural Science Foundation of Jiangsu Province (Grant Nos. BK20150170 and BK20171354), the Fundamental Research Funds for the Central Universities (Grant Nos. 2242017K40189 and 2242016K41001), Jiangsu key laboratory for advanced metallic materials (Grant No. BM2007204).

References

[1] J.W. Yeh, S.K. Chen, S.J. Lin, J.Y. Gan, T.S. Chin, T.T. Shun, et al., Nanostructured high-entropy alloys with multiple principal elements: novel alloy design concepts and outcomes, Adv. Eng. Mater. 6 (2004) 299–303.
[2] S. Singh, N. Wanderka, B.S. Murty, U. Glatzel, J. Banhart, Decomposition in multi-component AlCoCrCuFeNi high-entropy alloy, Acta Mater. 59 (2011) 182–190.
[3] J.Y. He, C. Zhu, D.Q. Zhou, W.H. Liu, T.G. Nieh, Z.P. Lu, Steady state flow of the FeCoNiCrMn high entropy alloy at elevated temperatures, Intermetallics 55 (2014) 9–14.
[4] Y. Zhang, T.T. Zuo, Z. Tang, M.C. Gao, K.A. Dahmen, P.K. Liaw, et al., Microstructures and properties of high-entropy alloys, Prog. Mater. Sci. 61 (2014) 1–93.
[5] S.F. Zhao, Y. Shao, X. Liu, N. Chen, H.Y. Ding, K.F. Yao, Pseudo-quinary $Ti_{20}Zr_{20}Hf_{20}Be_{20}(Cu_{20-x}Ni_x)$ high entropy bulk metallic glasses with large glass forming ability, Mater. Des. 87 (2015) 625–631.
[6] J.T. Huo, L.S. Huo, J.W. Li, H. Men, X.M. Wang, A. Inoue, et al., High-entropy bulk metallic glasses as promising magnetic refrigerants, J. Appl. Phys. 117 (2015) 073902.
[7] J.T. Huo, L.S. Huo, H. Men, X.M. Wang, A. Inoue, J.Q. Wang, et al., The magnetocaloric effect of Gd-Tb-Dy-Al-M (M = Fe, Co and Ni) high-entropy bulk metallic glasses, Intermetallics 58 (2015) 31–35.
[8] P.Y. Li, G. Wang, D. Ding, J. Shen, Glass forming ability, thermodynamics and mechanical properties of novel Ti-Cu-Ni-Zr-Hf bulk metallic glasses, Mater. Des. 53 (2014) 145–151.
[9] H.F. Li, X.H. Xie, K. Zhao, Y.B. Wang, Y.F. Zheng, W.H. Wang, et al., In vitro and in vivo studies on biodegradable CaMgZnSrYb high-entropy bulk metallic glass, Acta Biomater. 9 (2013) 8561–8573.
[10] V.K. Pecharsky, K.A. Gschneidner Jr., Giant magnetocaloric effect in $Gd_5(Si_2Ge_2)$, Phys. Rev. Lett. 78 (1997) 4494–4497.
[11] V.K. Pecharsky, K.A. Gschneidner Jr., Magnetocaloric effect and magnetic refrigeration, J. Magn. Magn Mater. 200 (1999) 44–56.
[12] H. Fu, X.Y. Zhang, H.J. Yu, B.H. Teng, X.T. Zu, Large magnetic entropy change of Gd-based ternary bulk metallic glass in liquid-nitrogen temperature range, Solid State Commun. 145 (2008) 15–17.
[13] L. Liang, X. Hui, G.L. Chen, Thermal stability and magnetocaloric properties of GdDyAlCo bulk metallic glasses, Mater. Sci. Eng. B 147 (2008) 13–18.
[14] Y.S. Liu, J.C. Zhang, Y.Q. Wang, Y.Y. Zhu, Z.L. Yang, J. Chen, et al., Weak exchange effect and large refrigerant capacity in a bulk metallic glass $Gd_{0.32}Tb_{0.26}Co_{0.20}Al_{0.22}$, Appl. Phys. Lett. 94 (2009) 112507.
[15] F. Yuan, J. Du, B.L. Shen, Controllable spin-glass behavior and large magnetocaloric effect in Gd-Ni-Al bulk metallic glasses, Appl. Phys. Lett. 101 (2012) 032405.
[16] J. Du, Q. Zheng, E. Brück, K.H.J. Buschow, W.B. Cui, W.J. Feng, et al., Spin-glass behavior and magnetocaloric effect in Tb-based bulk metallic glass, J. Magn. Magn Mater. 321 (2009) 413–417.
[17] Q. Luo, D.Q. Zhao, M.X. Pan, W.H. Wang, Magnetocaloric effect of Ho-, Dy-, and Er-based bulk metallic glasses in helium and hydrogen liquefaction temperature range, Appl. Phys. Lett. 90 (2007) 211903.
[18] L. Liang, X. Hui, C.M. Zhang, G.L.A. Chen, Dy-based bulk metallic glass with high thermal stability and excellent magnetocaloric properties, J. Alloy. Comp. 463 (2008) 30–33.
[19] K.L. Edwards, E. Axinte, L.L. Tabacaru, A critical study of the emergence of glass and glassy metals as “green” materials, Mater. Des. 50 (2013) 713–723.
[20] H.S. Chen, Thermal and mechanical stability of metallic glass ferromagnets, Scripta Metall. 11 (1977) 367–370.
[21] H.S. Chen, J.T. Krause, E. Coleman, Elastic constants, hardness and their implications to flow properties of metallic glasses, J. Non-Cryst. Solids 18 (1975) 157–171.
[22] J. Du, Q. Zheng, Y.B. Li, Q. Zhang, D. Li, Z.D. Zhang, Large magnetocaloric effect and enhanced magnetic refrigeration in ternary Gd-based bulk metallic glasses, J. Appl. Phys. 103 (2008) 023918.
[23] Q. Luo, M.B. Tang, J. Shen, Tuning the magnetocaloric response of Er-based metallic glasses by varying structural order in disorder, J. Magn. Magn Mater. 401 (2016) 406–411.
[24] H.Y. Zhang, R. Li, L.L. Zhang, T. Zhang, Tunable magnetic and magnetocaloric properties in heavy rare-earth based metallic glasses through the substitution of similar elements, J. Appl. Phys. 115 (2014) 133903.
[25] K.H.J. Buschow, Intermetallic compounds of rare-earth and 3d transition metals, Rep. Prog. Phys. 40 (1977) 1179.
[26] J.Y. Fan, L.S. Ling, B. Hong, L. Zhang, L. Pi, Y.H. Zhang, Critical properties of the perovskite manganite $La_{0.1}Nd_{0.6}Sr_{0.3}MnO_3$, Phys. Rev. B 81 (2010) 144426.
[27] H. Maletta, W. Felsch, Insulating spin-glass system $Eu_xSr_{1-x}S$, Phys. Rev. B 20 (1979) 1245.
[28] Q.Y. Dong, B.G. Shen, J. Chen, J. Shen, J.R. Sun, Spin-glass behavior and magnetocaloric effect in melt-spun TbCuAl alloys, Solid State Commun. 151 (2011) 112–115.
[29] K.A. Gschneidner Jr., V.K. Pecharsky, Magnetocaloric materials, Annu. Rev. Mater. Sci. 30 (2000) 387–429.
[30] D. Sherrington, S. Kirkpatrick, Solvable model of a spin-glass, Phys. Rev. Lett. 35 (1975) 1792–1796.